Photoluminescence from Defects in Be-doped GaN

M. A. Reshchikov*

Department of Physics, Virginia Commonwealth University, Richmond, VA 23220, USA

B. McEwen and F. Shahedipour-Sandvik

College of Nanoscale Science and Engineering, SUNY Polytechnic Institute, Albany, NY 12203, USA

Keywords: GaN, luminescence, defects, Be doping

Abstract

While GaN is a crucial semiconductor material for bright light-emitting devices, fabrication of *p*-type GaN remains challenging since the Mg acceptor commonly used for *p*-type doping is not shallow enough. Doping of GaN with Be is a promising path, yet no reliable *p*-type GaN has been achieved by Be doping so far. One of the reasons is a poor understanding of point defects in Be-doped GaN that can be studied by photoluminescence (PL). The yellow (YL_{Be}) band at 2.15 eV is the dominant PL band in Be-doped GaN. In this work, we discovered a blue PL band named the BL_{Be} band. It has a maximum at 2.6 eV and a lifetime of 0.8 μs at temperatures below 100 K. The BL_{Be} band is observed in GaN samples with relatively high concentrations of Be ($>10^{18}$ cm^{-3}). Both the YL_{Be} and BL_{Be} bands likely originate from the isolated Be_{Ga} defect, namely from electron transitions via the –/0 and 0/+ thermodynamic transition levels of the Be_{Ga}. The 0/+ transition level is located at 0.1-0.2 eV above the valence band. We also observed other broad PL bands in Be-doped GaN that are preliminarily attributed to Be-containing complexes.

*) mreshchi@vcu.edu

I. Introduction

GaN-based semiconductor materials are widely used in light-emitting devices and other applications.[1-4] Magnesium (Mg) is currently the only known viable acceptor for achieving low-resistivity *p*-type material in these devices. Yet, its use in AlGaN alloys is limited by relatively large ionization energy (E_A = 0.22 eV in GaN, and it increases with increasing Al content in AlGaN). Beryllium (Be) was proposed as an alternative to Mg in *p*-type doping of GaN [5-7] and AlN.[8,9] Early studies suggested that Be substituting for Ga (Be_{Ga}) is responsible for the shallow ultraviolet luminescence (UVL_{Be}) band with a sharp peak at 3.38 eV and that it is the shallowest acceptor in GaN with an ionization energy of 0.11 eV.[10-13] However, more recent studies indicated that the 3.38 eV band is likely caused by the $Be_{Ga}O_NBe_{Ga}$ complex acting as an acceptor in GaN.[14] At the same time, the isolated Be_{Ga} is a dual-nature acceptor[15] with three –/0 levels: at 0.24±0.02 eV (labeled Be3), 0.33±0.05 eV (Be1) and 0.38±0.03 eV (Be2) above the valence band maximum (VBM) in the limit of low temperatures.[16,17] A hole at the Be3 level is delocalized, whereas holes at the Be2 and Be1 levels are localized at the nearest N atom in the 0001 direction of the wurtzite lattice (Be2) or one of the three remaining equivalent in-plane directions (Be1). Note that recent first-principles calculations by others,[18-21] using the HSE hybrid functional, predicted only polaronic states of the Be_{Ga} acceptor with transition levels at 0.55-0.80 eV above the VBM (our calculations in Ref. 16 predicted 0.58 eV).

It is known that defects may have more than one charge transition level in the gap. The C_N defect in GaN is one of the best examples. In agreement with theoretical predictions,[22] the C_N defect has the –/0 level at 0.916±0.003 eV and the 0/+ level at 0.33±0.01 eV above the VBM.[23,24] Electron transitions via the –/0 and 0/+ levels cause the YL1 and BL_C bands with maxima at 2.17 and 2.85 eV, respectively, in C-doped GaN. In *n*-type GaN:C, the BL_C intensity increases

superlinearly with excitation intensity P_{exc} because the C_N must capture two holes before radiative recombination occurs. The BL_C can be called the secondary PL band of the C_N defect.

In this paper, we present plausible evidence that a new PL band with a maximum at 2.6 eV in Be-doped GaN (called hereafter the BL_{Be} band) is the secondary PL band of the Be_{Ga} defect.

2. Results

2.1. Three Types of GaN:Be Samples

In low-temperature steady-state PL (SSPL) spectra of GaN:Be samples (**Figure 1**) the near-band-edge (NBE) emission with a main peak at about 3.47 eV and its LO phonon replica at 3.38 eV were attributed to the donor-bound exciton.[25,26] At lower photon energies, the Be-related UVL_{Be} band with the ZPL at ~3.38 eV, the Mg_{Ga}-related UVL_{Mg} band with the ZPL at ~3.28 eV (several LO phonon replicas follow both the 3.38 and 3.28 eV peaks), and the broad YL_{Be} band with a maximum at about 2.15 eV were observed. In all GaN:Be samples, the YL_{Be} band, assigned to a deep polaronic state of the Be_{Ga} acceptor,[16] was the strongest defect-related PL band with the internal quantum efficiency (IQE) approaching unity in some samples.

To resolve broad overlapped PL bands, we used deconvolution of PL spectra based on the known shapes of well-studied PL bands. The shapes of the defect-related PL bands were fitted with the following expression obtained in a one-dimensional configuration coordinate model.[27]

$$I^{PL}(\hbar \quad \hbar \quad \left[-2S_e \left(\sqrt{\frac{E_0^* - \hbar}{d_{FC}^g}} \quad 1 \right)^2 \right] \qquad (1)$$

Here, S_e is the Huang-Rhys factor in the excited state of the defect, $d_{FC}^g = E_0^* - \hbar$ is the Frank-Condon shift in the ground state, $E_0^* = E_0 + 0.5\hbar$, E_0 is the zero-phonon line (ZPL)

energy, $\hbar$ is the energy of the effective phonon mode in the excited state, $\hbar$ and $\hbar$ are the photon energy and position of the PL band maximum, respectively. The Δ is a small shift of the PL band maximum due to sample-dependent reasons such as in-plane biaxial strain in thin GaN layers grown on sapphire substrates or local electric fields.

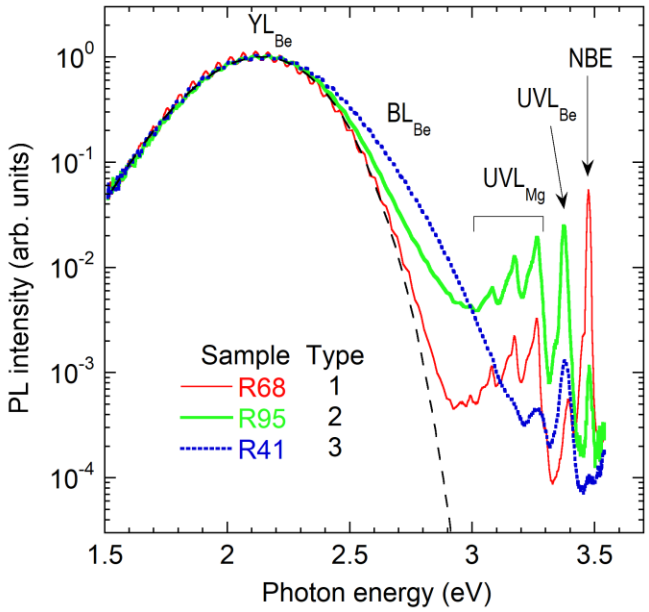

Figure 1. Normalized PL spectra from selected GaN:Be samples at T = 18 K and P_{exc} = 10^{-4} W/cm^2. The dashed line is calculated using Equation (1) with the following parameters: S_e = 22, E_0^* = 3.2 eV, $\hbar\omega_{max}$ = 2.15 eV. A weak peak at 3.39 eV for sample R68 is the LO phonon replica of the donor-bound exciton peak (labeled NBE), whereas peaks at about 3.37 eV for samples R41 and R95 are attributed to the UVL_{Be} band.

Concerning the YL_{Be} band shape, PL spectra from many GaN:Be samples can be formally divided into three types (**Table 1**). Representative PL spectra are shown in Figure 1.

Table 1. Parameters of GaN:Be samples grown by metal-organic chemical vapor deposition (MOCVD). Conductivity type: *n*, *p*, or semi-insulating (SI) as determined from PL, Hall effect, and hot probe (HP) measurements. Peak PL intensities are given in relative units, all divided by P_{exc} (given in W/cm^2 units in parentheses). The secondary-ion mass-spectrometry (SIMS) detection limit for [Be] is ~10^{17} cm^{-3}.

Type	Sample number	Be flow (nmol/min)	[Be] $\times 10^{18}$	Conductivity type	UVL_{Be} (0.13)	BL_{Be} (100)	NBE (10^{-4})	NBE (0.13)	YL1 (10^{-4})
1	R25	455	0.8	*n* (PL, Hall)	–		0.5	1	0.4
	R26	1000	0.8	*n* (PL, Hall)	–		0.1	0.4	0.4
	R27	1370	6	*n* (PL, Hall)	–		1	4	0.2
	R28	910	4	SI (PL)	0.2	0.04	0.01	1	0.01
	R55	455	1.5	SI (PL)	0.3	<0.02	0.01	3	
	R56	501	1	SI (PL)	–	<0.01	0.8	200	0.1
	R57	455	3	SI (PL)	0.1	<0.04	0.2	40	0.02
	R59	910	0.1	SI (PL)	–		10	70	
	R60	910	0.1	SI (PL)	–		40	120	
	R62	137	0.1	SI (PL)	–		2	80	0.2
	R68	455	1	SI (PL)	–		1	100	0.05
	R80	910	3	SI (PL)	–		0.2	8	
	R89	910	~3	*p* (HP)	0.3	0.05	0.03	5	
	R96	910	3	SI (PL)	0.02		0.2	100	
2	R77	910	3	SI (PL)	0.7	0.04	1	60	
	R78	910	4	SI (PL)	3	1.1	0.01	2	
	R79	1140	4	*p* (HP, Hall)	2	1	0.01	1	
	R81	910	3	SI PL)	1	0.1	0.01	1	
	R82	910	20	SI (PL)	4	1	0.01	0.4	
	R87	910	4	*p* (HP)	0.4	0.5	0.06	30	0.01
	R95	910	3	SI (PL)	1	0.3	0.01	4	
	R134	910	~3	*p* (Hall)	3	1	0.04	10	–
	R169	910	10	SI (PL)	2	1	0.02	9	
	R170	910	12	SI (PL)	1.5	1	0.001	0.15	
	R172	910	18		3	1	0.05	20	
3	R29	557	5	SI (PL)	15	1.1	0.001	0.2	–
	R39	3010	20	*p* (HP)	0.3	1.5	0.3	1	–
	R40	3010	30	*p* (HP, Hall)	2.5	1	0.001	0.05	–
	R41	3010	20	*p* (HP)	1	1	0.001	0.01	–
	R45	1370	20	SI (PL)	3	2.6	0.001	0.6	–
	R48	455	1	*p* (HP)	2	1.1	0.003	3	–
	R49	557	5	SI (PL)	3	3.8	0.002	1	–
	R54	464	7	*p* (HP, Hall)	3	1.5	0.01	0.8	–
	R182	910	6		2.4	0.2	0.02	3	

Below, the main characteristics of PL from these three groups are briefly reviewed. Note that the division into the three types is nominal and depends on the detection limit for resolving additional PL bands in GaN:Be samples.

Type 1 (sample R68 in Figure 1). The YL_{Be} band has a "normal" shape that did not change with variation of excitation intensity. It can be fitted using Equation (1) with the following parameters: S_e = 22-24, $\hbar\omega_{max}$ = 2.15 eV, and E_0^* = 3.2 eV. The UVL_{Be} band is absent or weak in these samples, whereas the NBE band is usually strong and often increases linearly with P_{exc}. All *n*-type samples (R25, R26, and R27) fall into this group, yet it also contains semi-insulating samples.

Type 2 (sample R95 in Figure 1). The YL_{Be} band has a "normal" shape in the limit of low P_{exc}, whereas a new PL band (the BL_{Be} band with a maximum at 2.6 eV) emerges as the YL_{Be} intensity saturates at high P_{exc}. The BL_{Be} band shape is the same in time-resolved PL (TRPL) and SSPL, and it can be fitted using Equation (1) with the following parameters: S_e = 12, $\hbar\omega_{max}$ = 2.6 eV, and E_0^* = 3.4 eV. The BL_{Be} band in SSPL is quenched at $T > 100$ K, revealing the activation energy of the quenching $E_A \approx 0.15$ eV. The NBE emission is very weak in these samples, increasing as $(P_{exc})^m$ with m = 1.5-2. It was found from the temperature-dependent Hall effect measurements and hot-probe measurements that at least some samples in this group (R79 and R134) are resistive *p*-type.[28] The PL from samples of this type always showed the UVL_{Be} band along with the BL_{Be} band.

Type 3 (sample R41 in Figure 1). A shoulder to the YL_{Be} band at the high energy side is observed even in the limit of low P_{exc}. Typical representatives are samples R39, R40, R41, R48, and R49. The PL spectra from all type-3 samples contain the UVL_{Be} band, and the concentration of Be from SIMS measurements is typically very high in these samples. Deconvolution of PL

spectra from type-3 samples reveals an additional PL band, with a maximum at ~2.45 eV (temporarily labeled GL_{Be}). Similar to type-2 samples, with increasing P_{exc} in SSPL experiments, the BL_{Be} band in these samples emerges superlinearly with P_{exc} when the YL_{Be} band saturates, and the fast component in TRPL experiments (0.7-0.8 μs) reveals the shape of the BL_{Be} band. Interestingly, the slow, nonexponential component repeats the SSPL shape with the high-energy shoulder (unresolved YL_{Be} and GL_{Be} bands). The NBE emission is very weak, and its intensity increases superlinearly with P_{exc} (similar to type-2 samples). Most of these samples showed *p*-type behavior in hot-probe measurements. Two samples (R40 and R54) were confirmed to be *p*-type with the Hall effect measurements.[28]

PL spectra from type-1 samples (containing only the YL_{Be} band at $\hbar\omega < 3.0$ eV at low temperatures) were studied in detail earlier.[16,17,29] Below, the additional Be-related PL bands (the BL_{Be} band at 2.6 eV and the GL_{Be} band at 2.45 eV), which appear in type 2 and 3 samples, will be analyzed in detail.

2.2. The BL_{Be} Band

2.2.1. Steady-State Photoluminescence

Figure 2 shows low-temperature SSPL spectra from a type-2 sample at three excitation intensities. With increasing P_{exc}, the YL_{Be} intensity saturates at $P_{exc} > 0.001$ W/cm^2. Concurrently, the BL_{Be} band with a maximum at 2.6 eV emerges at the high-energy side of the YL_{Be} band with increasing P_{exc}. These two PL bands are sufficient to explain PL spectra in a wide range of P_{exc}. In contrast to the YL_{Be} band, no significant saturation of the BL_{Be} band could be observed up to $P_{exc} \approx 100$ W/cm^2. From a comparison of the intensities of the YL_{Be} and BL_{Be} bands with the PL intensities from calibrated GaN samples, we estimated that the highest internal quantum efficiencies of these PL bands in our SSPL experiments are about 1 and 0.03, respectively.

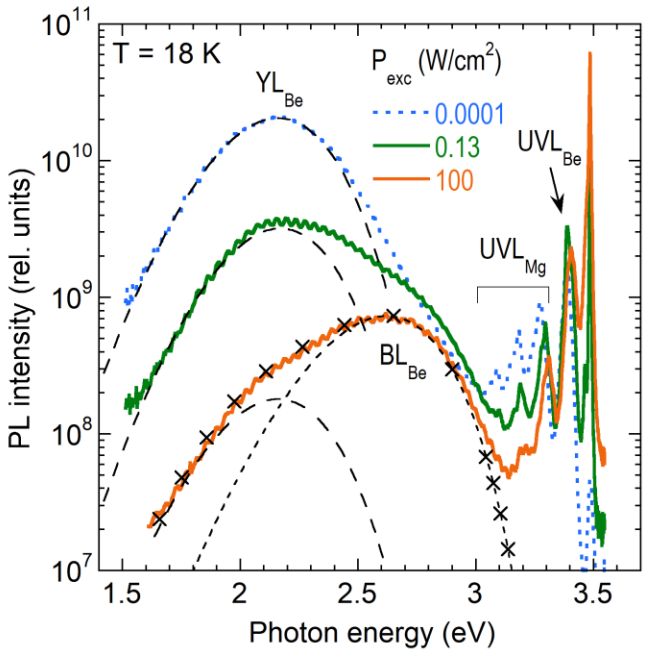

Figure 2. PL spectra divided by excitation intensity at T = 18 K for GaN:Be sample R172. The dashed lines are calculated using Equation (1) with the following parameters: S_e = 23, E_0^* = 3.2 eV, $\hbar\omega_{max}$ = 2.15 eV for the YL_{Be} band, and S_e = 12, E_0^* = 3.4 eV, $\hbar\omega_{max}$ = 2.60 eV for the BL_{Be} band. The × symbols show the sum of the calculated curves for the YL_{Be} and BL_{Be} bands at P_{exc} = 100 W/cm^2.

2.2.2. Time-Resolved Photoluminescence

In all the samples where the BL_{Be} band could be detected, the PL decay at photon energies close to 2.6 eV is exponential at T = 18 K. The PL lifetime is τ = 0.75±0.15 μs in all the samples. This indicates that the BL_{Be} band is caused by internal transitions.[30] Indeed, at such low temperatures, only two types of defect-related transitions in nondegenerate GaN are observed in PL experiments: electron transitions from shallow donors to acceptors always demonstrate nonexponential PL decay after a laser pulse, while internal transitions (from an excited state to the ground state) are typical for positively-charged donors and always show an exponential PL decay.[30] **Figure 3** shows PL decays at T = 18 K and selected photon energies. At $\hbar\omega$ = 2.7 eV, the PL decay is purely

exponential up to a few μs. In contrast, at $\hbar\omega = 1.75$ eV, the PL decay is nonexponential, close to the power dependence, $I^{PL}(t) = t^{-n}$ with $n \approx 0.8$ in a wide range of time delays, at least up to $t = 10^{-3}$ s (not shown in Figure 3). The PL decay at $\hbar\omega = 2.0$ eV contains both components.

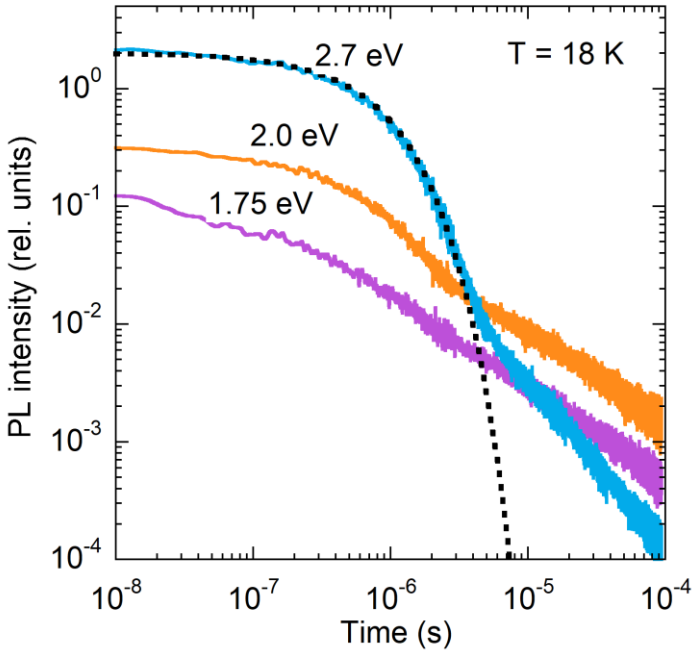

Figure 3. PL decays at selected photon energies at $T = 18$ K for GaN:Be sample R172. The dotted line is calculated using the following equation: $I^{PL} = I^{PL}(0)\exp(-t/\tau_0)$ with $\tau_0 = 0.75$ μs.

TRPL spectra at time delays of 0.5 and 50 μs are shown in **Figure 4**. One can see that the fast exponential component ($\tau \approx 0.7$ μs) originates from the BL_{Be} band, and the slow nonexponential component belongs to the YL_{Be} band.

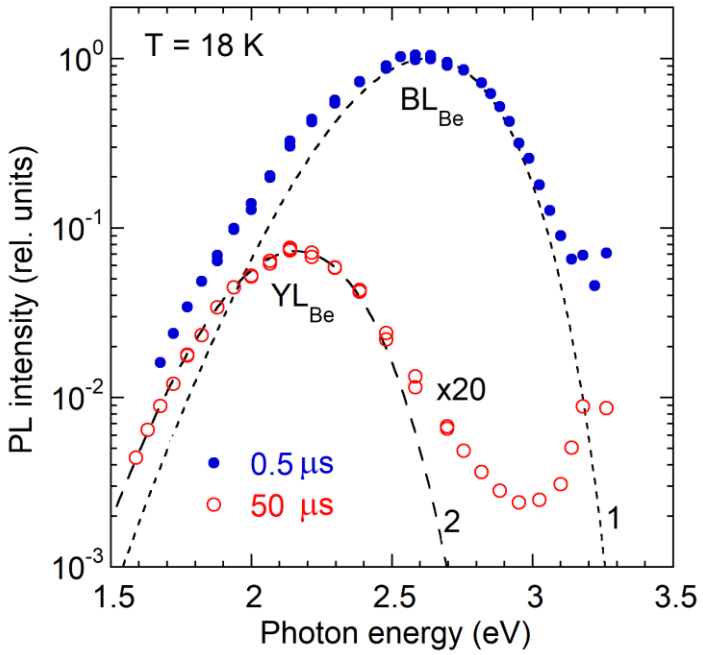

Figure 4. TRPL spectra for GaN:Be sample R172 at t = 0.5 μs (filled symbols) and t = 50 μs (empty symbols) at T = 18 K and $P_0 = 5\times10^{23}$ cm^{-2}s^{-1}. The data at 50 μs is multiplied by 20. The dashed lines are calculated using Equation (1) with the following parameters: S_e = 12, E_0^* = 3.4 eV, $\hbar\omega_{max}$ = 2.60 eV (1) and S_e = 24, E_0^* = 3.2 eV, $\hbar\omega_{max}$ = 2.15 eV (2).

We also analyzed the dependences of the peak PL intensities after a laser pulse on excitation intensity. **Figure 5** shows the $\eta(P)$ dependences for the YL$_{Be}$ and BL$_{Be}$ bands where η is the absolute IQE ($\eta = I^{PL}/P$) and P is the photon flux expressed in cm^{-2}s^{-1}. For the BL$_{Be}$ band, the maximum IQE (about 0.1) was estimated from comparison with a calibrated GaN:Zn,Si sample, in which $\eta > 0.9$ for the Zn-related blue band with similar PL lifetime (0.6 μs).[31] The absolute IQE for the YL$_{Be}$ band could not be estimated from TRPL measurements because its decay is nonexponential, and its approximate value (close to 1) was obtained from a comparison of SSPL spectra from GaN:Be and GaN:Zn,Si samples measured in identical conditions. The YL$_{Be}$ intensity increases linearly with P (constant η) up to ~10^{22} cm^{-2}s^{-1}. Above a critical photon flux (P_0) the

YL_{Be} band begins to exhibit saturation behavior (η decreases with P). The PL saturation is due to a limited number of defects, and the concentration of these defects can be found as [32]

$$N = \alpha \eta t_L P_0, \tag{2}$$

where α is the absorption coefficient (~10^5 cm^{-1} for GaN at 3.68 eV), η is the PL band's IQE before saturation, and t_L is the laser pulse duration (1 or 3 ns in our experiments). For the YL_{Be} band, $P_0^{YL} \approx 5\times10^{21}$ $cm^{-2}s^{-1}$ and $\eta^{YL} \approx 1$, which results in $N^{YL} \approx 10^{18}$ cm^{-3}.

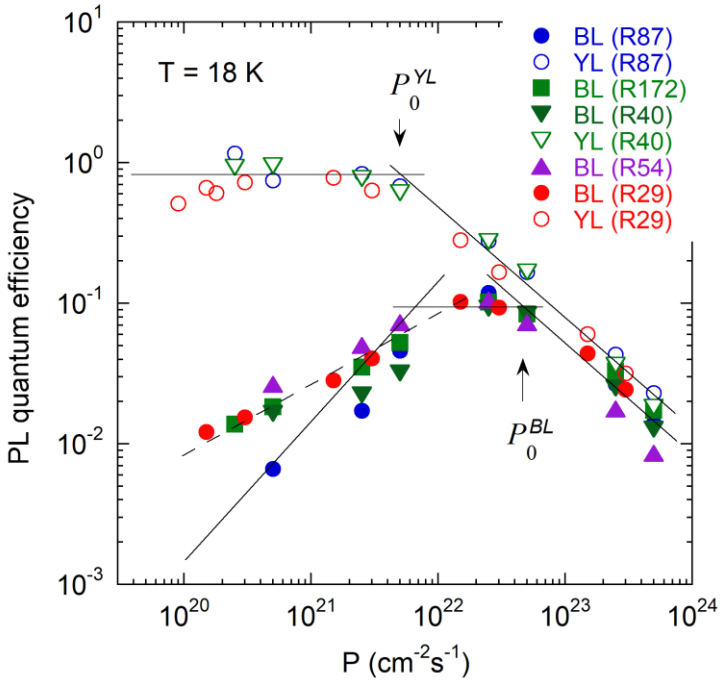

Figure 5. Dependences of TRPL IQE on excitation intensity at $T = 18$ K for selected GaN:Be samples. At $P < P_0^{YL} \approx 5\times10^{21}$ $cm^{-2}s^{-1}$, the YL_{Be} intensity (at $\hbar\omega = 2.2$ eV) increases linearly with P ($\eta \approx 1$) while the BL_{Be} intensity (at $\hbar\omega = 2.7$ eV) increases superlinearly (the dashed and solid lines show the $\eta \propto P^{1/2}$ and $\eta \propto P$ dependences, respectively). The saturation of the BL_{Be} band begins at $P = P_0^{BL} \approx 5\times10^{22}$ $cm^{-2}s^{-1}$. The lines are guides to eyes.

The BL_{Be} intensity increases superlinearly at $P < P_0^{YL} \approx 5\times10^{21}$ $cm^{-2}s^{-1}$, and its saturation begins at $P_0^{BL} \approx 5\times10^{22}$ $cm^{-2}s^{-1}$. From Equation (2) with $\eta^{BL} = 0.1$ we find $N^{BL} \approx 10^{18}$ cm^{-3} . Note

that the accuracy of these estimates is low (plus-minus half an order of magnitude) because of difficulties in finding the absolute IQE of PL and the simplified model of PL.[30-32]

The superlinear $I^{PL}(P)$ dependence for the BL_{Be} band at $P < 5\times10^{21}$ $cm^{-2}s^{-1}$ ($I^{PL} \propto P^m$ with m = 1.5-2) is similar to observed dependences for the BL3 and GL1 (also known as GL) bands in GaN grown by hydride vapor phase epitaxy (HVPE)[33,34] and the BL_C band in GaN:C.[23] Such behavior is typical for a "secondary" PL band, which requires two holes to be captured by a defect before PL occurs. The GL1 band is caused by an unknown defect in HVPE-grown GaN that captures two holes to produce the green PL (in Ref. [33], we erroneously attributed it to the 0/+ level of the C_N defect). The BL3 band is attributed to the RY3 defect, which is likely related to the Fe_{Ga}. The BL_C band is caused by transitions via the 0/+ level of the C_N defect.[23] The behavior of the YL_{Be} and BL_{Be} bands in Figure 5 seems consistent with their attribution to the –/0 and 0/+ levels of the Be_{Ga} acceptor with a concentration of ~10^{18} cm^{-3}, although more statistical data are needed for the convincing conclusion.

2.2.3. Temperature Dependences

With increasing temperature, the BL_{Be} intensity in samples from groups 2 and 3 did not change up to $T \approx 100$ K. At higher temperatures, SSPL quenching with an activation energy of about 0.10-0.15 eV was observed for P_{exc} = 12-100 W/cm^2 [**Figure 6** and **7(a)**]. The temperature dependence of PL lifetime, $\tau(T)$, was nearly identical to the $I^{PL}(T)$ dependence for the BL_{Be} band in the SSPL experiment [**Figure 7(b)**].

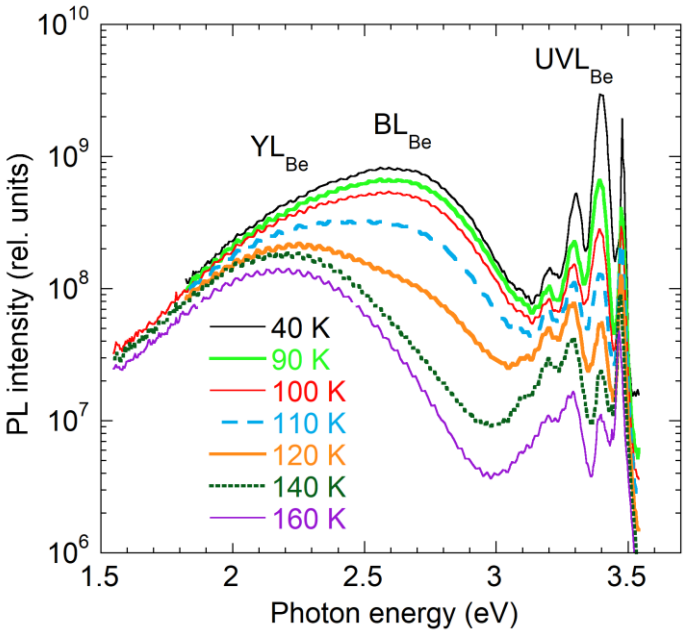

Figure 6. PL spectra at selected temperatures for GaN:Be sample R170 at P_{exc} = 100 W/cm^2.

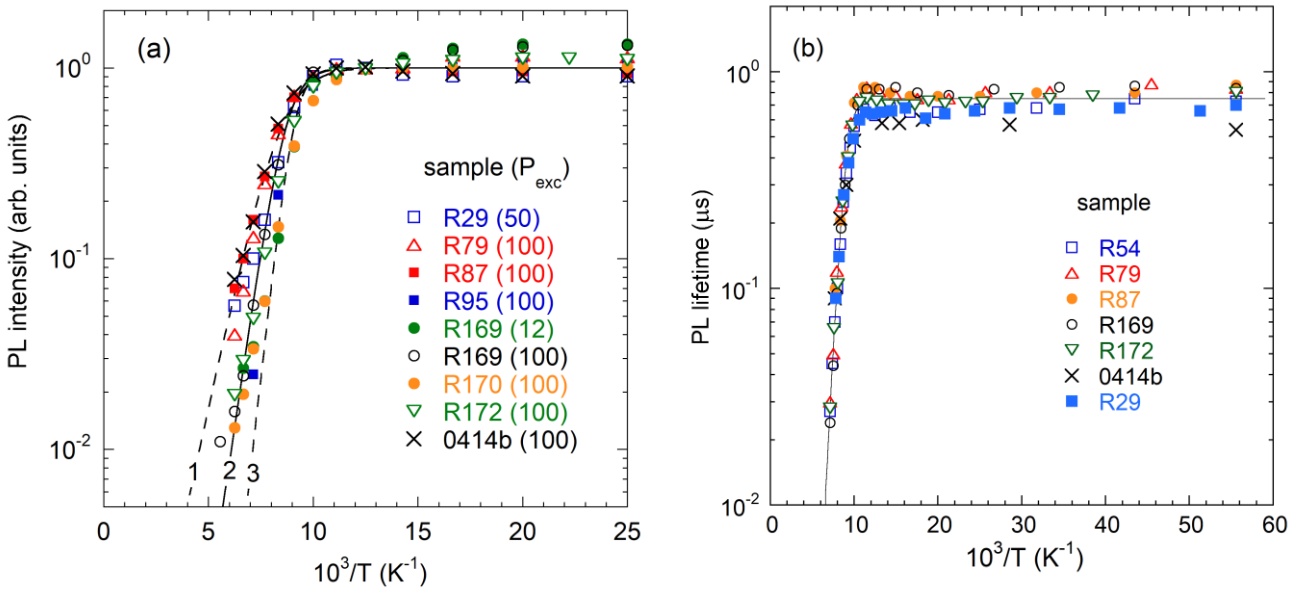

Figure 7. Temperature dependences of the BL_{Be} intensity and lifetime in selected GaN:Be samples. (a) normalized PL intensities, (b) PL lifetime at 2.7-2.8 eV. The lines in (a) are calculated using Equation (3) with the following parameters: E_A = 100 meV, $C = 2\times10^4$ (1), E_A = 150 meV, $C = 4\times10^6$ (2), E_A = 200 meV, $C = 1.5\times10^9$ (3). The line in (b) is calculated using Equation (3) and (4) with the following parameters: E_A = 130 meV, τ_0 = 0.75 μs, $C_p = 6\times10^{-7}$ cm^3/s, $(1-\eta_0) \approx 1$.

The $I^{PL}(T)$ and $\tau(T)$ dependences can be fitted with the following expression:[30]

$$\frac{I^{PL}(T)}{I^{PL}(0)} = \frac{\eta(T)}{\eta_0} = \frac{\tau(T)}{\tau_0} = \frac{1}{1 + C\exp\left(\frac{-E_A}{kT}\right)} \quad (3)$$

Here, $I^{PL}(0)$, η_0, and τ_0 are the PL intensity, IQE, and PL lifetime, respectively, at temperatures before the quenching begins, and k is Boltzmann's constant. For the $I^{PL}(T)$ dependence in conductive n-type GaN, parameter E_A is the defect ionization energy (the distance from the defect level to the valence band) and

$$C = (1-\eta_0)\tau_0 C_p N_v g^{-1}, \quad (4)$$

where N_v is the effective density of states in the valence band (we assumed $N_v = N_v' T^{3/2}$ with N_v' = 3.15×10^{15} cm^{-3}K$^{-3/2}$ for GaN), g is the degeneracy of the defect level (assumed $g = 2$), and C_p is the hole-capture coefficient for the defect. In semi-insulating GaN, the defect-related PL is usually quenched by the abrupt and tunable quenching mechanism,[35] i.e., PL intensity abruptly drops (with a slope much larger than E_A/k) at a critical temperature T_0, and T_0 increases with increasing P_{exc}. In such a case, the $I^{PL}(T)$ dependence can still be formally fitted with Equation (3), yet parameters C_p and E_A will not have physical meaning. The abrupt and tunable quenching of PL is explained by the inverse population of levels in the gap of a semi-insulating semiconductor (acceptors become saturated with photogenerated holes and donors – with electrons) at $T < T_0$, which abruptly switches to equilibrium population at $T \approx T_0$ due to thermal emission of holes from the acceptor to the valence band.[35] In contrast to the $I^{PL}(T)$ dependence in the SSPL experiment, the $\tau(T)$ dependence in *both* conductive and semi-insulating GaN can be fitted with Eqs. (3) and (4),[30,36] see Figure 7(b) for SI and p-type GaN:Be and Ref. [29] for n-type GaN:Be, and parameters C_p and E_A can be found (given in the figure caption). This can be explained by the

assumption that the inverse population is not achieved in our TRPL measurements in contrast to the SSPL conditions.

Interestingly, the quenching of the BL_{Be} band in the SSPL experiment is tunable but *not abrupt*. This is typical for defects with levels close to the valence band.[37] Similar behavior was observed for the BL2 and UVL_{Be} bands caused by the C_NH_i and $Be_{Ga}O_NBe_{Ga}$ defects, respectively.[14,38] In this case, the slope of the quenching reveals the ionization energy E_A. Overall, from SSPL and TRPL dependences, we estimate that $E_A = 0.15\pm0.05$ eV for the BL_{Be} band.

2.3. PL Bands in Type-3 GaN:Be Samples

2.3.1. Steady-State Photoluminescence

In low-temperature PL spectra of type-3 samples a noticeable shoulder at the high-energy side of the YL_{Be} band is observed already at very low P_{exc} (sample R41 in Figure 1). With increasing P_{exc} the shoulder rises and eventually develops into the BL_{Be} band with a maximum at 2.6 eV (**Figure 8**). However, unlike the case of type-2 samples, the PL spectra cannot be deconvoluted by using shapes of only the YL_{Be} and BL_{Be} bands. In the assumption that the shapes of PL bands are the same in different samples, and in order to keep the minimum number of components in the deconvolution, we will add one more band, with a maximum at ~2.4 eV, and temporarily call it the GL_{Be} band due to its location in the green part of the spectrum. In contrast to the YL_{Be} and BL_{Be} bands, the shapes of which can be reliably found at least under certain experimental conditions (Figure 1,2,4 and 8), the GL_{Be} band is always buried under stronger PL bands. As a result, its shape and position remain uncertain. For simplicity, the GL_{Be} band shape in Figure 8 was simulated using a Gaussian curve with a maximum at 2.4 eV and fixed width. However, similar results could be obtained by using a shape given by Equation (1) with a wide range of fitting parameters.

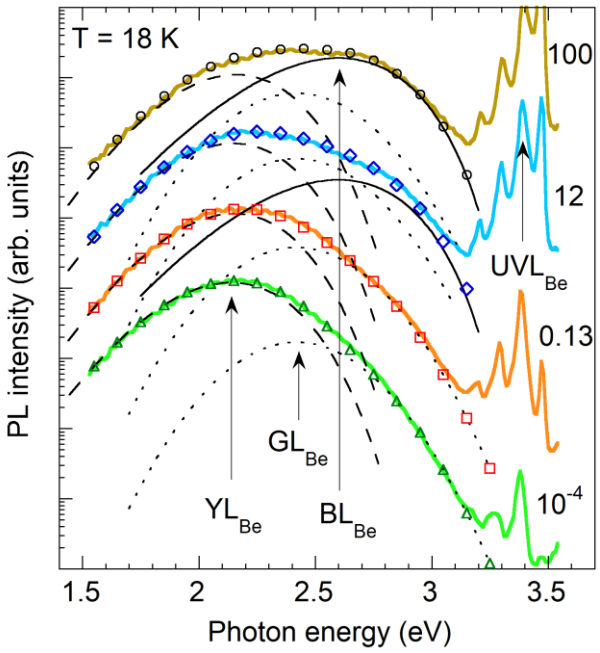

Figure 8. Evolution of low-temperature (18 K) SSPL spectrum with P_{exc} (given on the right side in W/cm^2) for the type-3 GaN:Be sample R41. The PL spectra are arbitrarily shifted vertically for clarity. The broad band is deconvoluted by using known shapes of the YL_{Be} (dashed curve) and BL_{Be} (solid curve) bands. An additional PL band with a maximum at about 2.42 eV (the GL_{Be} band shown with the dotted line) is needed for a perfect agreement of the sum of the components (YL_{Be} + GL_{Be} + BL_{Be}, shown with symbols) with the experimental PL shape between 1.5 and 3.0 eV.

With increasing P_{exc}, the YL_{Be} and GL_{Be} bands start saturating at P_{exc} > 0.1 W/cm^2, while the ratio of their intensities remains nearly constant up to P_{exc} = 100 W/cm^2 (Figure 8). The BL_{Be} (2.6 eV), UVL_{Be} (3.38 eV) and NBE (3.47 eV) intensities increase superlinearly with P_{exc} up to P_{exc} = 12 W/cm^2 and linearly at higher P_{exc}.

2.3.2. Time-Resolved Photoluminescence

As before, we tried to resolve components of the broad PL band between 1.5 and 3.2 eV by using TRPL. Examples of TRPL spectra for a type 3 sample at T = 18 K are shown in **Figure 9**. At small

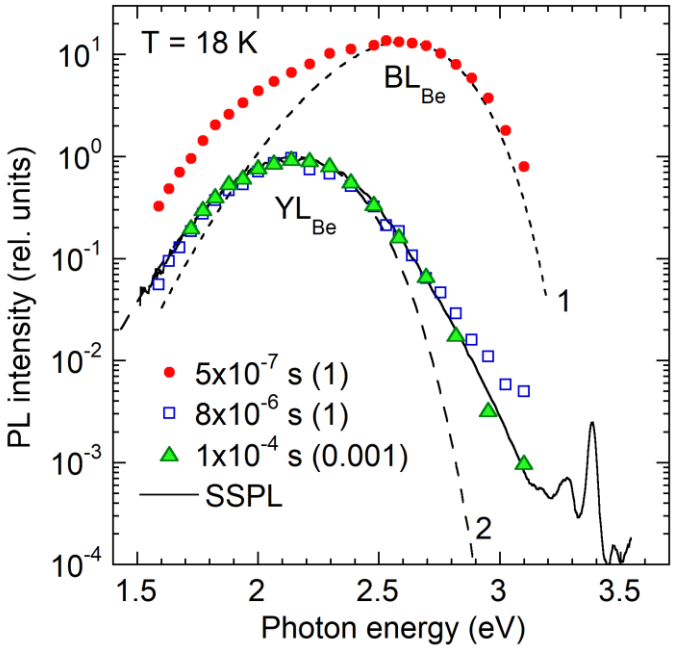

Figure 9. Low-temperature (18 K) TRPL spectra for GaN:Be sample R40 (type 3) at t = 0.5 μs and t = 8 μs ($P = 5\times10^{23}$ cm^{-2}s^{-1}) and at t = 100 μs ($P = 5\times10^{20}$ cm^{-2}s^{-1}). The intensity of the PL spectrum at 100 μs (green triangles) is multiplied by 100. The attenuation of P is shown in brackets. The dashed lines are calculated using Equation (1) with the following parameters: S_e = 12, E_0^* = 3.4 eV, $\hbar\omega_{max}$ = 2.60 eV (1) and S_e = 22, E_0^* = 3.2 eV, $\hbar\omega_{max}$ = 2.15 eV (2). The solid line shows an SSPL spectrum measured at low excitation intensity ($P_{exc} = 10^{-4}$ W/cm^2) and arbitrarily shifted vertically to match the TRPL spectra.

time delays, the BL_{Be} band dominates, and its decay is exponential at T = 18 K. At $t > 10^{-5}$ s, the BL_{Be} band disappears, and the YL_{Be} band decays nonexponentially at longer time delays (not shown in Figure 9). Interestingly, the high-energy shoulder to the YL_{Be} (supposedly the unresolved GL_{Be} band) remains at $t > 10^{-5}$ s, and the TRPL spectrum matches the SSPL spectrum (Figure 9). Sometimes, PL bands can be resolved in TRPL experiments if they have different decay rates after a laser pulse.[32] However, the YL_{Be} and supposed GL_{Be} bands remain unresolved when TRPL is measured at $P = 5\times10^{20}$ and 5×10^{23} cm^{-2}s^{-1} (Figure 9).

In MBE-grown GaN:Be samples, the BL_{Be} and GL_{Be} bands can also be found. **Figure 10** shows the evolution of low-temperature PL spectra with time after a laser pulse with high (a) and low (b) excitation intensities. At small time delays, the BL_{Be} band dominates, and its decay is exponential at $T = 18$ K (not shown). At $t > 10^{-5}$ s, the BL_{Be} band disappears, and the broad band is observed. Similar to PL spectra from our MOCVD GaN:Be samples of type 3, the shape of this band has a shoulder at the high-energy side that can be attributed to an additional GL_{Be} band with a maximum at about 2.45 eV.

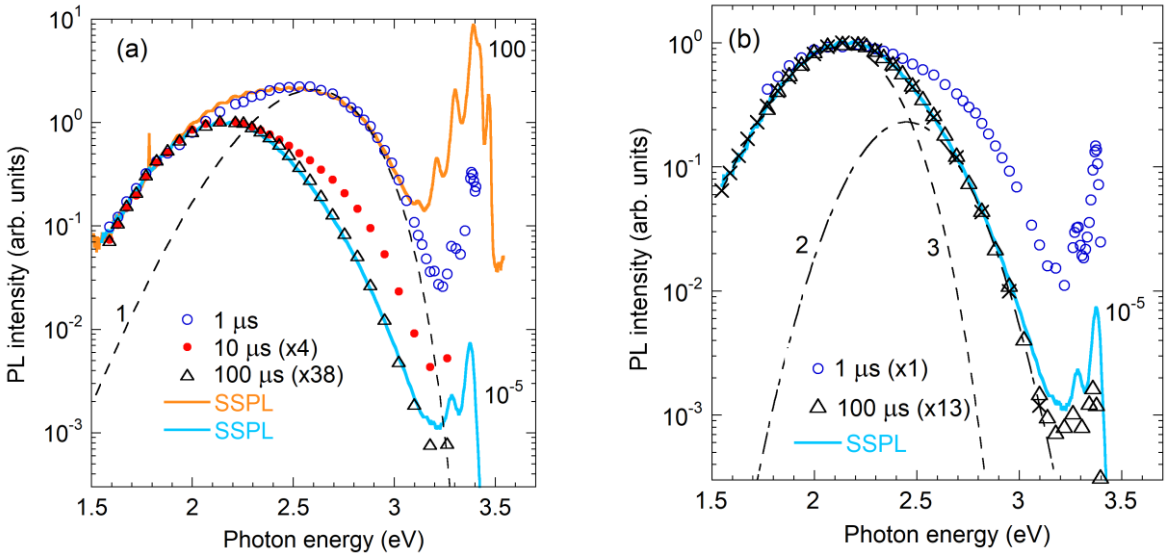

Figure 10. TRPL and SSPL spectra (normalized at the YL_{Be} maximum) at $T = 18$ K from MBE GaN:Be sample 0414b (type 3). SSPL: P_{exc} = 10^{-5} and 100 W/cm^2 (shown with numbers near SSPL spectra). TRPL: $P = 5\times10^{23}$ cm^{-2}s^{-1} (a) and $P = 5\times10^{20}$ cm^{-2}s^{-1} (b). The dashed lines 1 and 3 are calculated using Equation (1) with the following parameters: S_e = 12, E_0^* = 3.4 eV, $\hbar\omega_{max}$ = 2.6 eV (1), and S_e = 22, E_0^* = 3.2 eV, $\hbar\omega_{max}$ = 2.15 eV (3). The dash-dotted line 2 is a Gaussian curve with a maximum at 2.45 eV. The × symbols in (b) show the sum of the calculated curves 2 and 3.

2.3.3. Temperature Dependences

Figure 11 and **12** show the evolution of SSPL spectra with temperature in two MOCVD GaN:Be samples at selected excitation intensities. Deconvolution of these PL spectra reveals three Be-

related PL bands: the YL_{Be}, GL_{Be}, and BL_{Be}. **Figure 13** shows the Arrhenius plot for Be-related PL bands for one of the type-3 GaN:Be samples. The lines in Figure 13 are given as examples of the fits (not the best fits because of insufficient data points). The $I^{PL}(T)$ dependences for the UVL_{Be}, BL_{Be}, and YL_{Be} bands are the same as in samples of types 1 and 2. The data for the GL_{Be} are less certain because of the poor resolution of this band. Nevertheless, it is clear that its intensity is nearly constant up to ~200 K, after which it quenches together with the YL_{Be} band.

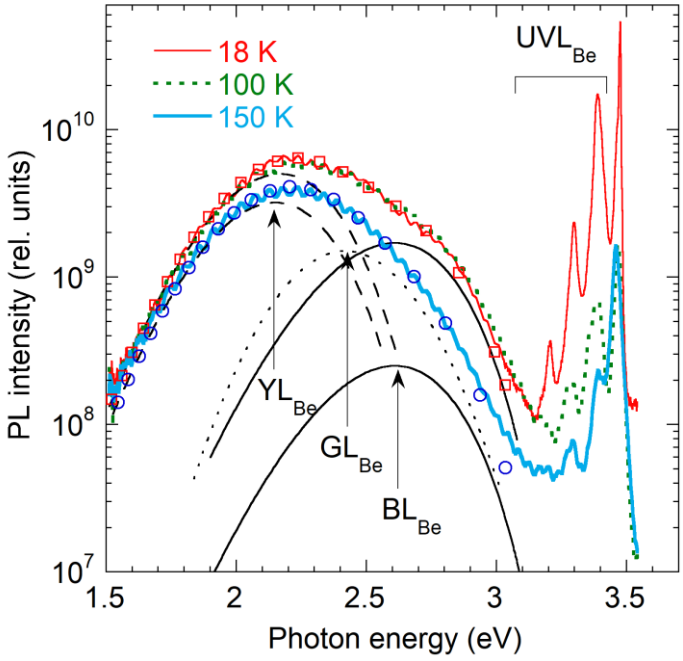

Figure 11. Evolution of SSPL spectrum with temperature at high excitation intensity (P_{exc} = 12 W/cm^2) for GaN:Be sample R41 (type 3). The broad band between 1.5 and 3.2 eV is deconvoluted by using known shapes of the YL_{Be} (dashed curve) and BL_{Be} (solid curve) and GL_{Be} (dotted line) components. The circles show the sums of three calculated curves.

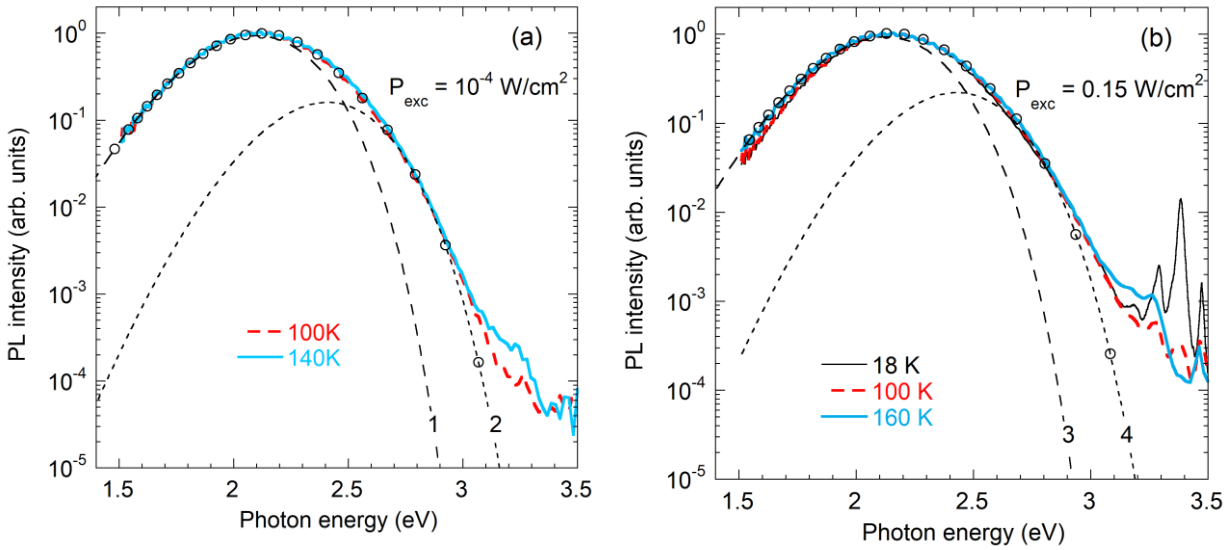

Figure 12. SSPL spectra at low excitation intensities and selected temperatures from MOCVD GaN:Be sample R39 (type 3). a) $P_{exc} = 10^{-4}$ W/cm^2, b) $P_{exc} = 0.15$ W/cm^2. The lines are calculated using Equation (1) with the following parameters: $S_e = 22$, $E_0^* = 3.2$ eV, $\hbar\omega_{max} = 2.15$ eV (1,3) and $S_e = 30$, $E_0^* = 3.6$ eV, $\hbar\omega_{max} = 2.43$ eV (2,4). The circles show sums of the two calculated curves.

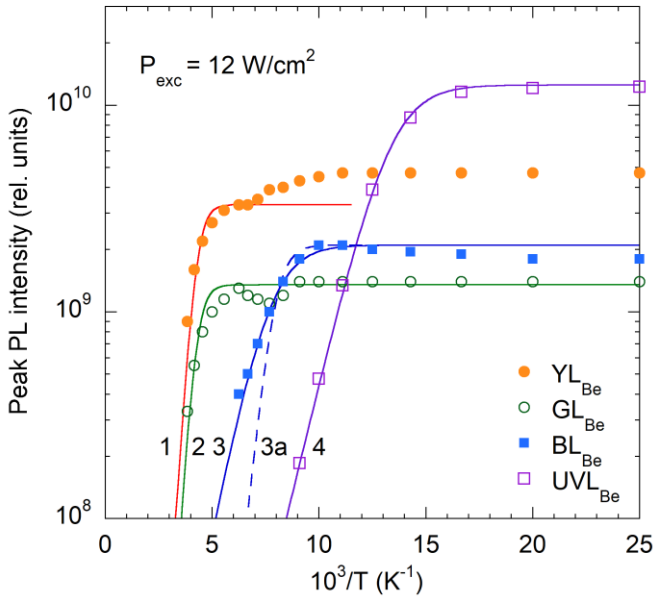

Figure 13. Temperature dependences of peak PL intensities at $P_{exc} = 12$ W/cm^2 for Be-related PL bands in GaN:Be sample R41 (the PL spectra are shown in Fig. 11). The lines are calculated using Equation (3) with the following parameters: $C = 3\times10^6$ (1,2), 1.8×10^3 (3), 1×10^8 (3a), and 5×10^5 (4), $E_A = 300$ meV (1,2), 100 meV (3), 200 meV (3a), and 85 meV (4).

3. Discussion

Figure 14 shows the charge transition levels and related electron transitions responsible for the Be-related PL bands in Be-doped GaN. The isolated Be_{Ga} acceptor, thanks to its dual nature, has three –/0 transition levels in the gap.[16] The shallow level at 0.24 eV with a delocalized hole is responsible for the UVL_{Be3} band with a maximum at 3.26 eV that can be observed only at $T >$ 130 K because a hole quickly relaxes to the deeper level over a small barrier at low temperatures. Two deep levels (at 0.38 and 0.33 eV) correspond to small polarons where a hole is localized on axial (Be2) and nonaxial (Be1) neighbor nitrogen atoms, respectively. These two levels are responsible for the broad YL_{Be} band with a maximum at 2.15 eV where the Be1 and Be2 components are not resolved but explain two-step quenching and a sudden shift of the YL_{Be} band at $T \approx$100 K.

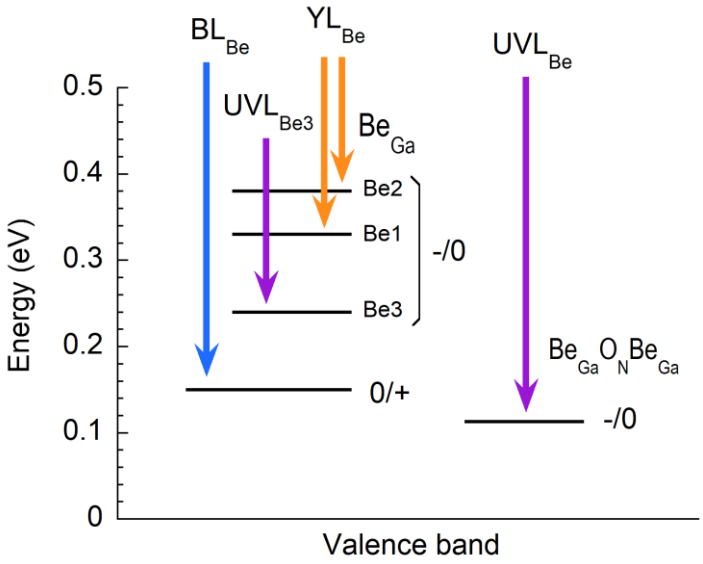

Figure 14. Energy levels of the Be_{Ga} defect responsible for the YL_{Be}, UVL_{Be3}, and BL_{Be} bands and the $Be_{Ga}O_NBe_{Ga}$ complex responsible for the UVL_{Be} band at 3.38 eV. The arrows show electron transitions from the conduction band (or from shallow donors) for the YL_{Be}, UVL_{Be3}, and UVL_{Be} bands and from an excited state close to the conduction band in the case of the BL_{Be}.

In the current work, we studied in detail the BL_{Be} band, which has a maximum at 2.6 eV. Its superlinear increase with excitation intensity (both in SSPL and TRPL experiments) suggests that it is likely a secondary PL band, i.e., the PL that requests a capture of two holes before radiative recombination takes place. Moreover, the decay of the BL_{Be} intensity after a laser pulse is exponential even at the lowest temperatures (down to 18 K), indicating that this PL is caused by an internal transition – from an excited state (presumably, close to the conduction band) to the ground state. Note that such behavior is a unique feature of all donors contributing to PL in GaN.[30] The superlinear increase of intensity and exponential decay of the BL_{Be} band can be explained by the assumption that it is caused by transitions of electrons from an excited state to the 0/+ ground state of the Be_{Ga} defect. This PL behavior is very similar to that of the C_N defect in GaN, the –/0 and 0/+ levels of which (at 0.915 and 0.33 eV, respectively, above the VBM) are responsible for the YL1 and BL_C bands with maxima at 2.17 and 2.85 eV, respectively.[23] From temperature dependences of PL intensity and PL lifetime, the position of the 0/+ level is estimated at 0.10-0.15 eV above the VBM for the BL_{Be} band. However, it is known that for several reasons, the slope of the PL quenching is typically smaller (by at least 20-40 meV) than the ionization energy of the defect.[30,36] An independent parameter that reveals the ionization energy is the critical temperature at which the PL quenching and the decrease of PL lifetime begin (T_0).[36] It follows that E_A = 0.15-0.20 eV from $T_0 \approx 110$ K. The shape of the Be_{Ga} band indicates that its ZPL is at 3.3-3.4 eV. From all these estimates we conclude that $E_A = 0.15 \pm 0.05$ eV for the 0/+ level of the Be_{Ga} defect. Note that current hybrid functional calculations of Be_{Ga} acceptor in GaN do not find the 0/+ transition level of this defect.[39] We think that the close location of this level to the valence band may be the reason why calculations fail to find it. Further theoretical and experimental studies, including complementary techniques, may resolve the apparent controversy.

The shape of the broad PL band in type-3 samples could be explained by the assumption that a weak green luminescence (GL_{Be}) band with a maximum at ~2.4 eV contributes at the high-energy side of a stronger YL_{Be} band but remains unresolved when temperature or excitation intensity are varied in SSPL and TRPL experiments. It was found only in samples with a high concentration of Be. It might be caused by some complex defect containing one or more Be atoms. Alternatively, the defects in close vicinity to the Be_{Ga} acceptor in heavily Be-doped GaN samples may modify its adiabatic potentials, which would distort the shape of the YL_{Be} band and create a shoulder.

Finally, PL spectra from Be-doped GaN contain the UVL_{Be} band with the strongest peak at 3.38 eV followed by LO phonon replicas. This PL band is caused by transitions of electrons from shallow donors (at $T < 50$ K) or from the conduction band ($T > 50$ K) to the shallow acceptor with the –/0 level at 0.113 eV above the VBM. We recently proposed that it is caused by the $Be_{Ga}O_NBe_{Ga}$ complex,[14] which is likely to form in semi-insulating or *p*-type GaN:Be during growth. First-principles calculations predict that the $Be_{Ga}O_NBe_{Ga}$ complex is a dual-nature acceptor with shallow and deep levels at 0.12 and 0.34 eV above the VBM.[14] However, only the shallow level could be found in our PL experiments. The UVL_{Be} band is detected only in samples with a relatively high concentration of Be (above 10^{18} cm^{-3}). It is likely that gallium vacancies, which should be abundant during MOCVD growth in N-rich conditions, assist the formation of the $Be_{Ga}O_NBe_{Ga}$ complexes. Indeed, the mobile V_{Ga} acceptors are attracted by the stationary O_N donors to form the $V_{Ga}O_N$ complexes, after which the mobile Be_i donors substitute for the V_{Ga} to form the $Be_{Ga}O_N$ complexes. These complexes are neutral (neither donors nor acceptors),[29] and can bind another V_{Ga}, which eventually is filled with the second Be atom.

Lastly, the red luminescence (RL_{Be}) band with a maximum at 1.8 eV was recently studied and attributed to the V_NBe_{Ga} complex.[40] It appears in GaN:Be samples grown by MBE and annealed

at 900 °C. Interestingly, we did not find the RL_{Be} band in GaN:Be samples grown by MOCVD, even after annealing these samples at temperatures up to 1000 °C. One reason for this is that our MOCVD samples were grown under N-rich conditions, hindering the formation of nitrogen vacancies and facilitating the formation of gallium vacancies, Be_{Ga} acceptors, and $Be_{Ga}O_NBe_{Ga}$ complexes. Besides, in *p*-type GaN:Be samples, where the Fermi level is pinned at the Be_{Ga} level (~0.35 eV above the VBM), the RL_{Be} band could not be observed even if the V_N and V_NBe_{Ga} defects are present and abundant. Indeed, the V_NBe_{Ga} complex is in the 2+ state in such samples, while the RL_{Be} band is caused by an internal transition (from an excited state close to the conduction band to the ground state at 0.6-0.9 eV above the VBM) involving the 0/+ charge transition level.[40]

4. Conclusion

The main PL band in low-temperature PL spectra from Be-doped GaN is the YL_{Be} band with a maximum at 2.15 eV attributed to the deep polaronic state of the Be_{Ga} acceptor with the –/0 transition level at 0.35±0.05 eV above the VBM. In this work, we observed the blue luminescence (BL_{Be}) band with a maximum of 2.6 eV and preliminarily assigned it to electron transitions via the 0/+ level of the Be_{Ga} defect located at 0.15±0.05 eV above the VBM. This attribution is supported by a superlinear increase of the BL_{Be} intensity with excitation intensity (because two holes must be captured by the Be_{Ga}) and purely exponential decay of the BL_{Be} intensity after a laser pulse with a PL lifetime of ~0.75 μs in all samples. The exponential decay of defect-related PL at such low temperatures as 18 K in nondegenerate GaN indicates that it is caused by electron transition from an excited state to the ground state of the defect, which is typical for donors in GaN. In GaN samples heavily doped with Be, the UVL_{Be} band is observed with the first peak at 3.38 eV. It is

attributed to the shallow state of the $Be_{Ga}O_NBe_{Ga}$ complex with the –/0 level at 0.113±0.002 eV above the VBM.

5. Experimental Section

5.1. Samples

Most of the samples studied in this work are ~500 nm-thick GaN:Be layers grown on unintentionally doped GaN on c-plane sapphire substrates in a vertical cold wall MOCVD reactor under N-rich conditions. More details about the growth can be found elsewhere.[41] The concentration of beryllium ([Be]) was measured by secondary ion mass spectroscopy (SIMS) and varied between 10^{18} and 3×10^{19} cm^{-3} (Table I). Three samples (R25-R27) were conductive *n*-type, in agreement with a relatively high concentration of oxygen ([O] = 1.1×10^{18} cm^{-3} for sample R26 from SIMS) due to contamination during MOCVD growth. The majority of GaN:Be samples were semi-insulating (SI), and *p*-type conductivity was found in nine samples by temperature-dependent (300-500 K) Hall effect measurements,[28] or by hot-probe (HP) measurements. The concentration of oxygen was measured in a few samples by SIMS, but the results were inconclusive. In particular, [O] = 3×10^{17} cm^{-3} for sample R29. In the SIMS profiles of samples R48 and R56 [O] gradually decreased from ~1×10^{18} cm^{-3} to 1×10^{17} cm^{-3} (which is our detection limit for oxygen) from the surface to 400-800 nm. Such tails in SIMS depth profiles are likely caused by secondary implantation of the surface contaminants.[42] The concentration of C is about 10^{17} cm^{-3} in our MOCVD GaN:Be samples, and a weak C_N-related yellow band could be detected in PL spectra of several samples at $T > 200$ K (Table 1). Sample 0414b is a Be-doped GaN layer with [Be] = 10^{21} cm^{-3} grown by molecular beam epitaxy (MBE) on the c-plane sapphire substrate at West Virginia University.[43] More details about the growth of MBE GaN:Be samples studied in this work can be found elsewhere.[12,29,43]

5.2. Photoluminescence Measurements

Steady-state PL (SSPL) was excited with an unfocused He-Cd laser (30 mW, 325 nm), dispersed by a 1200 rules/mm grating in a 0.3 m monochromator, and detected by a cooled photomultiplier tube. Calibrated neutral-density filters were used to attenuate the excitation power density (P_{exc}) over the range of 10^{-5} - 0.2 W/cm^2. For high excitation intensities, up to 100 W/cm^2, the laser beam was focused onto a ~0.1 mm diameter spot. A closed-cycle optical cryostat was used for temperatures between 15 and 320 K.

All the samples were studied under identical conditions, and the PL spectra were corrected for the spectral response of the measurement system. As in our other works after 2018, the PL spectra, $I^{PL}(\lambda)$, were additionally multiplied by λ^3 in order to plot the spectra in units proportional to the number of emitted photons as a function of photon energy.[30,44] The absolute internal quantum efficiency (IQE) of the PL from a particular defect, η, was estimated by comparing integrated PL intensity with the PL intensity obtained from calibrated GaN samples.[31,35]

The time-resolved PL (TRPL) was excited with a pulsed nitrogen laser (repetition frequency of 6 Hz, photon energy of 3.68 eV and pulse durations of 1 and 3 ns for two nitrogen lasers) and analyzed with a digital oscilloscope. The photon flux during the pulse, P, was varied between 3×10^{20} and 5×10^{23} cm^{-2}s^{-1} by using neutral density filters. The TRPL spectra were obtained from these transients at selected time delays. The stability of the signal was validated by measuring the PL decay at a characteristic photon energy (usually at the band maximum) before and after the PL spectrum measurement. Analyses of temperature-dependent SSPL and TRPL also allowed us to reliably distinguish *n*-type conductive GaN from semi-insulating (SI) GaN. In particular, abrupt and tunable quenching of PL is observed only in SI (or resistive *p*-type) GaN samples.[35]

Acknowledgments

The work at VCU and SUNY was partly supported by the National Science Foundation under grants DMR-2423874 and DMR-2423875, respectively.

Conflict of Interest

The authors declare no conflict of interest.

Data Availability Statement

The data that support the findings of this study are available from the corresponding author upon reasonable request.

References

[1] H. Morkoç, *Handbook of Nitride Semiconductors and Devices*, Wiley, New York, USA **2008**.

[2] S. J. Pearton, J. C. Zolper, R. J. Shul, and F. Ren, "GaN: Processing, defects, and devices", *J. Appl. Phys*. **1999**, 86, 1.

[3] G. Li, W. Wang, W. Yang, Y. Lin, H. Wang, Z. Lin, and S. Zhou, "GaN-based light-emitting diodes on various substrates: a critical review", *Rep. Prog. Phys.* **2016**, 79, 056501.

[4] E. A. Jones, F. Wang, and D. Costinett, "Review of Commercial GaN Power Devices and GaN-Based Converter Design Challenges", *IEEE J. Emerging Selected Topics in Electronics* **2016**, 4, 707.

[5] K. H. Ploog and O. Brandt, "Doping of group III nitrides", *J. Vac. Sci. Technol. A* **1998**, 16, 1609.

[6] T. M. Al Tahtamouni, A. Sedhain, J. Y. Lin, and H. X. Jiang, "Beryllium Doped p-type GaN Grown by Metal-Organic Chemical Vapor Deposition", *Jordan J. Phys*. **2010**, 3, 77.

[7] S. Sugita, Y. Watari, G. Yoshizawa, J. Sodesawa, H. Yamamizu, K.-T. Liu, Y.-K. Su, and Y. Horikoshi, "Growth of Be-doped p-type GaN under invariant polarity conditions", *Jpn. J. Appl. Phys.* **2003**, 42, 7194.

[8] H. Ahmad, J. Lindemuth, Z. Engel, C. M. Matthews, T. M. McCrone, and W. A. Doolittle, "Substantial P-Type Conductivity of AlN Achieved via Beryllium Doping", *Adv. Mater*. **2021**, 33, 2104497.

[9] W. A. Doolittle, C. M. Matthews, H. Ahmad, S. Lee, A. Ghosh, E. N. Marshall, A. L. Tang, P. Manocha, and D. Yoder, "Prospectives for AlN electronics and optoelectronics and the important role of alternative synthesis", *Appl. Phys. Lett*. **2023**, 123, 070501.

[10] F. J. Sánchez, F. Calle, M. A. Sánchez-García, E. Calleja, E. Muñoz, C. H. Molloy, D. J. Somerford, J. J. Serrano, and J. M. Blanco, "Experimental evidence for a Be shallow acceptor in GaN grown on Si(111) by molecular beam epitaxy**"**, *Semicond. Sci. Technol.* **1998**, 13, 1130.

[11] D. J. Dewsnip, A. V. Andrianov, I. Harrison, J. W. Orton, D. E. Lacklison, G. B. Ren, S. E. Hooper, T. S. Cheng, and C. T. Foxon, "Photoluminescence of MBE grown wurtzite Be-doped GaN", *Semicond. Sci. Technol.* **1998**, 13, 500.

[12] A. J. Ptak, T. H. Myers, L. Wang, N. C. Giles, M. Moldovan, C. R. D. Cunha, L. A. Hornak, C. Tian, R. A. Hockett, S. Mitha, and P. Van Lierde, "A Comparison of Magnesium and Beryllium Acceptors in GaN Grown by rf-Plasma Assisted Molecular Beam Epitaxy", *MRS Online Proceedings Library* **2000**, 639, 33. https://doi.org/10.1557/PROC-639-G3.3

[13] D. O. Demchenko, M. Vorobiov, O. Andrieiev, T. H. Myers, and M. A. Reshchikov, "Shallow and deep states of beryllium acceptor in GaN: Why photoluminescence experiments do not reveal small polarons for defects in semiconductors", *Phys. Rev. Lett.* **2021**, 126, 027401.

[14] M. A. Reshchikov, D. O. Demchenko, B. McEwen, and F. Shahedipour-Sandvik, "On the identity of the shallowest acceptor in GaN", *Phys. Rev. B* **2025**, 111, 045202.

[15] S. Lany and A. Zunger, "Dual nature of acceptors in GaN and ZnO: The curious case of the shallow MgGa deep state", *Appl. Phys. Lett*. **2010**, 96, 142114.

[16] M. A. Reshchikov, M. Vorobiov, O. Andrieiev, D. O. Demchenko, B. McEwen, and F. Shahedipour-Sandvik, "Dual Nature of the Be_{Ga} Acceptor in GaN: Evidence from Photoluminescence", *Phys. Rev. B* **2023**, 108, 075202.

[17] M. A. Reshchikov and M. Bockowski, "The Origin of the Yellow Luminescence Band in Bulk Be-doped GaN", *Solids* **2024**, 5, 29.

[18] J. L. Lyons, A. Janotti, and C. G. Van de Walle, "Impact of group-II acceptors on the electrical and optical properties of GaN", *Jap. J. Appl. Phys*. **2013**, 52, 08JJ04.

[19] X. Cai, J. Yang, P. Zhang, and S.-H. Wei, "Origin of Deep Be Acceptor Levels in Nitride Semiconductors: The Roles of Chemical and Strain Effects", *Phys. Rev. Appl*. **2019**, 11, 034019.

[20] S. Jin, X. Li, W. Yang, Y. Zhao, L. Bian, S. Lu, "Electrical and Optical Properties of Beryllium Deep Acceptors in GaN", *J. Electron. Mater*. **2020**, 49, 7472.

[21] S. Qiao, Y.-N. Wu, X. Yan, B. Monserrat, S.-H. Wei, and B. Huang, "Temperature effect on charge-state transition levels of defects in semiconductors", *Phys. Rev. B* **2022**, 105, 115201.

[22] J. L. Lyons, A. Janotti, and C. G. Van de Walle, "Effects of carbon on the electrical and optical properties of InN, GaN, and AlN", *Phys. Rev. B* **2014**, 89, 035204.

[23] M. A. Reshchikov, M. Vorobiov, D. O. Demchenko, Ü. Özgür, H. Morkoç, A. Lesnik, M. P. Hoffmann, F. Hörich, A. Dadgar, and A. Strittmatter, "Two charge states of the C_N acceptor in GaN: Evidence from photoluminescence", *Phys. Rev. B* **2018**, 98, 125207.

[24] M. A. Reshchikov "Fine Structure of the Carbon-Related Blue Luminescence Band in GaN", *Solids* **2022**, 3, 231.

[25] J. A. Freitas, Jr., W. J. Moore, B. V. Shanabrook, G. C. B. Braga, S. K. Lee, S. S. Park, and J. Y. Han, "Donor-related recombination processes in hydride-vapor-phase epitaxial GaN", *Phys. Rev. B* **2002**, 66, 233311.

[26] A. Wysmolek, M. Potemski, R. Stepniewski, J. M. Baranowski, D. C. Look, S. K. Lee, and J. Y. Han, "Resonant interaction of LO phononswith excited donor states in GaN", *Phys. Stat. Sol. B* **2003**, 235, 36.

[27] M. A. Reshchikov, D. O. Demchenko, J. D. McNamara, S. Fernández-Garrido, and R. Calarco, "Green luminescence in Mg-doped GaN", *Phys. Rev. B* **2014**, 90, 035207.

[28] M. Zajac, L. Konczewicz, M. A. Reshchikov, B. McEwen, and F. Shahedipour-Sandvik, "P-type conductivity in GaN:Be epitaxial layers", an abstract to the IWN-2024 conference, Honolulu, HI, November 3-8, 2024.

[29] M. Vorobiov, O. Andrieiev, D. O. Demchenko, and M. A. Reshchikov, "Point Defects in Beryllium Doped GaN", *Phys. Rev B* **2021**, 104, 245203.

[30] M. A. Reshchikov, "Measurement and analysis of photoluminescence in GaN", *J. Appl. Phys*. **2021**, 129, 121101.

[31] M. A. Reshchikov, M. A. Foussekis, J. D. McNamara, A. Behrends, A. Bakin, and A.Waag, "Determination of the absolute internal quantum efficiency of photoluminescence in GaN co-doped with Zn and Si", *J. Appl. Phys*. **2012**, 111, 073106.

[32] M. A. Reshchikov, "Time-resolved photoluminescence from defects in GaN", *J. Appl. Phys*. **2014**, 115, 103503.

[33] M. A. Reshchikov, D. O. Demchenko, A. Usikov, H. Helava, and Yu. Makarov, "Carbon defects as sources of the yellow and green luminescence bands in undoped GaN", *Phys. Rev. B*, **2014**, 90, 235203.

[34] M. A. Reshchikov, "Fine structure of another blue luminescence band in undoped GaN", *Appl. Phys. Lett*. **2019**, 115, 262102.

[35] M. A. Reshchikov, A. A. Kvasov, M. F. Bishop, T. McMullen, A. Usikov, V. Soukhoveev, and V. A. Dmitriev, "Tunable and abrupt thermal quenching of photoluminescence in high-resistivity Zn-doped GaN", *Phys. Rev. B* **2011,** 84, 075212.

[36] M. A. Reshchikov, "Photoluminescence from defects in GaN", Gallium Nitride Materials and Devices XVIII, ed. H. Fujioka, H. Morkoç, and U. Schwarz, *Proc. SPIE, Gallium Nitride Materials and Devices XVIII*, **2023**, 12421,1242109. Doi: 10.1117/12.2645878

[37] M. A. Reshchikov, "Mechanisms of thermal quenching of defect-related luminescence in semiconductors", *Phys. Stat. Sol. A* **2020**, 218, 2000101.

[38] M. A. Reshchikov, O. Andrieiev, M. Vorobiov, B. McEwen, F. Shahedipour-Sandvik, D. Ye, and D. O. Demchenko, "Stability of the C_NH_i complex and the BL2 luminescence band in GaN", *Phys. Stat. Sol. B* **2021**, 258, 2100392.

[39] D. Demchenko, Private communication.

[40] M. Vorobiov, O. Andrieiev, D. Demchenko, and M. A. Reshchikov, "Nitrogen vacancy-acceptor complexes in GaN" *J. Appl. Phys*. **2024**, 135, 155701.

[41] M. A. Reshchikov, M. Vorobiov, O. Andrieiev, B. McEwen, E. Rocco, V. Meyers, D. O. Demchenko, and F. Shahedipour-Sandvik, "Photoluminescence from Be-Doped GaN Grown by Metal-Organic Chemical Vapor Deposition", *Phys. Stat. Sol. B* **2023**, 260, 202200487.

[42] M. A. Reshchikov, M. Vorobiov, A. Andrieiev, K. Ding, V. Avrutin, A. Usikov, H. Helava, and Yu. Makarov, "Determination of the concentration of impurities in GaN from photoluminescence and secondary-ion mass spectrometry", *Scientific Reports* **2020**, 10, 2223.

[43] K. Lee, "Issues for p-type doping of gallium nitride with beryllium and magnesium grown by rf-plasma assisted molecular beam epitaxy", Ph.D. dissertation, West Virginia University, West Virginia, USA (2007).

[44] I. Pelant and J. Valenta, *Luminescence Spectroscopy of Semiconductors*, Oxford Univ. Press, Oxford, UK, p. 61, **2012**.